Si− and Zn−doping of lattice matched $B_xIn_zGa_{1-x-z}As$− and $In_xGa_{1-x}N_yAs_{1-y}$−layers

Gunnar Leibiger [1], ***Claudia Krahmer*** [1], Volker Gottschalch [1], Gabriele Benndorf [2], Volker Riede [2]

1) Dept. of Inorganic Chemistry/Semiconductor Chemistry Group/University of Leipzig/Linnestr. 3, 04103 Leipzig, Germany , 2) Dept. of Experimental Physics II/University of Leipzig/Linnestr. 5, 04103 Leipzig, Germany

Introduction

$In_xGa_{1-x}N_yAs_{1-y}$−alloys have attained great attention in the past few years due to the possibility of lattice matched or strained growth on GaAs substrates in combination with a large reduction of the band−gap energy with increasing nitrogen incorporation [1]. Highly strained $In_xGa_{1-x}N_yAs_{1-y}$−layers with large In contents have been used as active material in 1.3−1.5 µm laser diodes [2]. Lattice matched layers are of high interest for high−efficiency multi−junction solar cells [3]. The new $B_xIn_zGa_{1-z}As$−material system, which is largely unknown, offers new possibilities in band−gap engineering and strain reduction [4,5]. The growth of lattice matched $B_xIn_zGa_{1-z}As$−layers on GaAs has also been demonstrated introducing the material as another candidate for solar−cell applications [4,5]. Systematic doping studies are prerequisite for application of both materials in solar cells or detector structures. However, systematic doping investigations of $B_xIn_zGa_{1-z}As$ and $In_xGa_{1-x}N_yAs_{1-y}$ using metalorganic vapour−phase epitaxy (MOVPE) are either absent or very rare, respectively [6]. In this work, we investigate the Si− and Zn−doping of lattice matched $B_xIn_zGa_{1-z}As$− and $In_xGa_{1-x}N_yAs_{1-y}$−layers using MOVPE and disilane and diethylzinc as doping precursors. All layers were characterized with high−resolution x−ray diffraction, photoluminescence (PL), Hall−measurements and infrared spectroscopic ellipsometry (IR−SE).

Experimental

$B_xIn_zGa_{1-z}As$− and $In_xGa_{1-x}N_yAs_{1-y}$−layers have been grown lattice matched on (001)−GaAs substrates at 550°C and 560°C, respectively using low−pressure (p_{tot} = 50 mbar) MOVPE (AIX200). The total flow into the horizontal reactor amounted to 7ssl and the growth rate was ~ 800 nm/min. Triethyl boron (TEB), (1,1)−dimethyl hydrazine (DMHy), trimethyl gallium (TMGa), trimethyl indium (TMIn), diethyl zinc (DEZn) and disilane (500 ppm in H_2) were used as B−, N−, Ga−, In−, Zn− and Si−precursors, respectively. Tertiarybutyl arsine (TBAs) and arsine were used as As−precursor for the growth of $In_xGa_{1-x}N_yAs_{1-y}$ and $B_xIn_zGa_{1-z}As$, respectively. The nitrogen− and indium compositions of the approximately 1 µm thick, lattice matched $In_xGa_{1-x}N_yAs_{1-y}$−layers can be estimated to y = 0.016 and x = 0.047 and the band−gap energy is ~1.08 eV. The compositions and the band−gap energy of the lattice matched $B_xIn_zGa_{1-z}As$−layers (d ~ 1 µm) amount to x @ 0.027, z @ 0.06 and E_g = 1.36 eV. The partial pressures of TMIn, TMGa, DMHy, and TBAs, used for the growth of $In_xGa_{1-x}N_yAs_{1-y}$, were $1.158*10^{-4}$, $2.6980*10^{-3}$, $1.9*10^{-1}$, and $1.293*10^{-2}$ mbar, respectively. The partial pressures of TEB, TMIn, TMGa, and arsine, used for the growth of $B_xIn_zGa_{1-z}As$, amounted to $4.95*10^{-3}$, $1.365*10^{-4}$, $2.7146*10^{-3}$, and $7.117*10^{-1}$ mbar, respectively.

Results

Nominally undoped $In_xGa_{1-x}N_yAs_{1-y}$−layers were found to be p−type with free hole concentrations ranging from ~ 6×10^{16} cm^{-3} (V/III = 25) to ~ 2×10^{16} cm^{-3} for V/III−rations above 100. In comparison, the background−doping level was drastically reduced for the $B_xIn_zGa_{1-z}As$−layers, for which free electron concentrations of 10^{10} cm^{-3} (V/III = 41) and 5×10^{13} cm^{-3} (V/III = 8) have been measured. These values are surprisingly low in view of the relatively large boron−carbon bondstrength.

Fig. 1 (a) shows the free carrier concentrations of the Si−doped $In_xGa_{1-x}N_yAs_{1-y}$− and $B_xIn_zGa_{1-x-z}As$ − layers resulting from the Hall−measurements as a function of the normalized partial pressure of disilane in the gasphase. With increasing Si−incorporation, the p−type $In_xGa_{1-x}N_yAs_{1-y}$−layers become semiinsulating and for

$p_{disilane}/p_{group-III}$−values above 10^{-3}, *n*−type conduction is obtained with a maximum electron concentration of ~6×10^{18} cm^{-3} for $p_{disilane}/p_{group-III}$ = 0.1. For normalized disilane−partial pressures between 0.007 and 0.07, the increase of the electron concentration is approximatively linear and a Si−distribution coefficient k_{Si} of ~0.004 can be estimated. Please note that in this

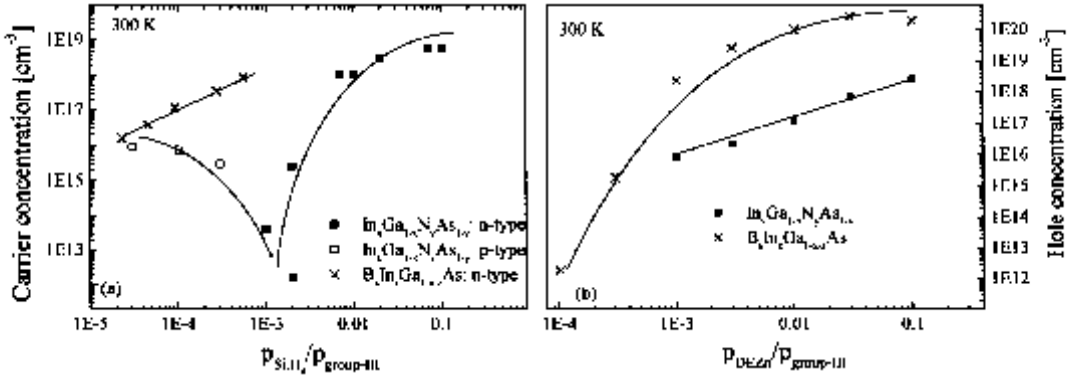

Fig. 1: (a): Free carrier concentration of Si-doped $In_xGa_{1-x}N_yAs_{1-y}$- (squares) and $B_xIn_zGa_{1-z}As$-layers (crosses) depending on the ratio of the partial pressure of disilane to the partial pressures of all group-III precursors. (b): Free hole concentration of Zn-doped $In_xGa_{1-x}N_yAs_{1-y}$- (squares) and $B_xIn_zGa_{1-z}As$-layers (crosses) depending on the ratio of the partial pressure of DEZn to the partial pressures of all group-III precursors. All lines are shown to guide the eye.

approximation autocompensation effects and the formation of Si−precipitates (both observed in Si−GaAs [7]) are neglected. For $B_xIn_zGa_{1-z}As$, the Si−doping efficiency is clearly increased compared to $In_xGa_{1-x}N_yAs_{1-y}$ (for $2.2\times10^{-5} < p_{disilane}/p_{group-III} < 5.5\times10^{-4}$), which can be understood by the smaller compensation ratio in $B_xIn_zGa_{1-z}As$. The electron concentration increases linearly with increasing $p_{disilane}/p_{group-III}$−ratio and a Si−distribution coefficient k_{Si} of 0.075 can be estimated under the same assumptions as for $In_xGa_{1-x}N_yAs_{1-y}$. This value is significantly enhanced compared to $In_xGa_{1-x}N_yAs_{1-y}$ (k_{Si} ~ 0.004), which might be partly due to the increased autocompensation ratio and/or tendency for formation of Si−precipitates for higher Si−concentrations [7].

Incorporation of Zn resulted in *p*−type conduction for both materials, $In_xGa_{1-x}N_yAs_{1-y}$ and $B_xIn_zGa_{1-z}As$ (Fig. 1 (b)). In Ref. 6, *n*−type conduction was obtained for Zn−doped $In_xGa_{1-x}N_yAs_{1-y}$ using MOVPE under similar growth conditions. The origin of this puzzling difference remains unsolved and needs further clarification. For $In_xGa_{1-x}N_yAs_{1-y}$, we obtain linearly increasing hole concentrations with increasing $p_{DEZn}/p_{group-III}$−ratio up to the highest obtained value of $p \sim 3\times10^{18}$ cm^{-3} and a Zn−distribution coefficient k_{Zn} of ~ 0.012 can be estimated. In comparison, the Zn−doping efficiency is drastically enhanced in $B_xIn_zGa_{1-z}As$. Assuming that all Zn−atoms are incorporated on group−III lattice sites, a Zn−distribution coefficient k_{Zn} of ~ 0.4 can be estimated for $p_{DEZn}/p_{group-III}$−ratios between 0.001 and 0.03, where the incorporation behaviour is approximately linear. Different surface reconstructions and the higher As/group−III−ratio in $B_xIn_zGa_{1-z}As$ leading to a higher number of group−III vacancies might explain the observed differences between the two materials.

Fig. 2 shows the Hall−mobilities of the Si− (a) and Zn−doped (b) $In_xGa_{1-x}N_yAs_{1-y}$− (squares) and $B_xIn_zGa_{1-z}As$−layers (crosses) as a function of the carrier concentration. Generally, the mobilities of the $B_xIn_zGa_{1-z}As$−layers are clearly enhanced (by a factor 2−5) compared to the corresponding values for $In_xGa_{1-x}N_yAs_{1-y}$, which can be explained by the lower compensation ratio in $B_xIn_zGa_{1-z}As$. For *n*−type layers, there is a trend of increasing mobilities with decreasing electron concentrations for high Si−compositions (Fig. 2 (a)). This can be understood by the decreasing number of ionized impurities with decreasing Si−concentration. The saturation or even decrease of the mobilities in the low−concentration region hints at a second process, possibly the

interaction of the Si−dopants with other defects, which may

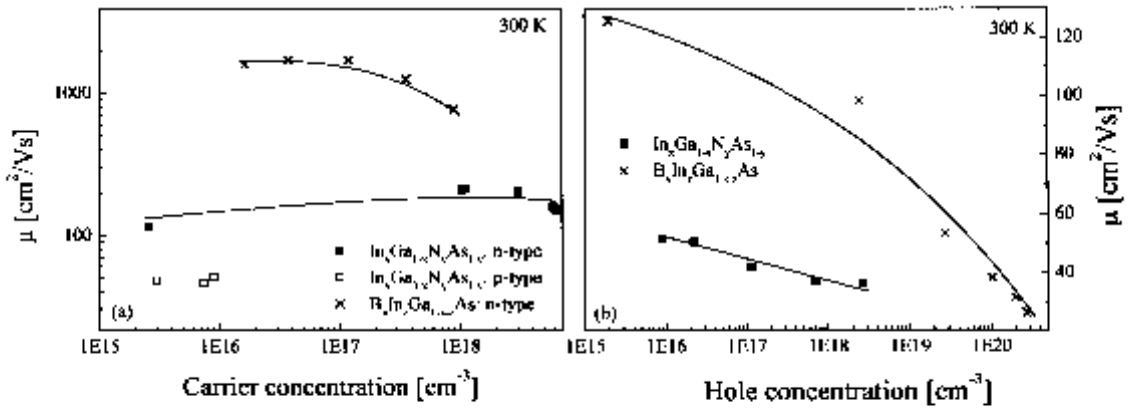

Fig. 2: (a): Hall-mobility of Si-doped $In_xGa_{1-x}N_yAs_{1-y}$- (squares) and $B_xIn_zGa_{1-z}As$-layers (crosses) depending on the carrier concentration. (b): Hall-mobility of Zn-doped $In_xGa_{1-x}N_yAs_{1-y}$- (squares) and $B_xIn_zGa_{1-z}As$-layers (crosses) depending on the hole concentration. All lines are shown to guide the eye.

also be concluded from PL−experiments (see below). The mobilities of both types of Zn−doped layers decrease with increasing Zn−concentration due to enhanced ionized−impurity scattering and are generally lower than the mobilities of the Si−doped samples, which is due to the higher valence−band effective masses (Fig. 2 (b)).

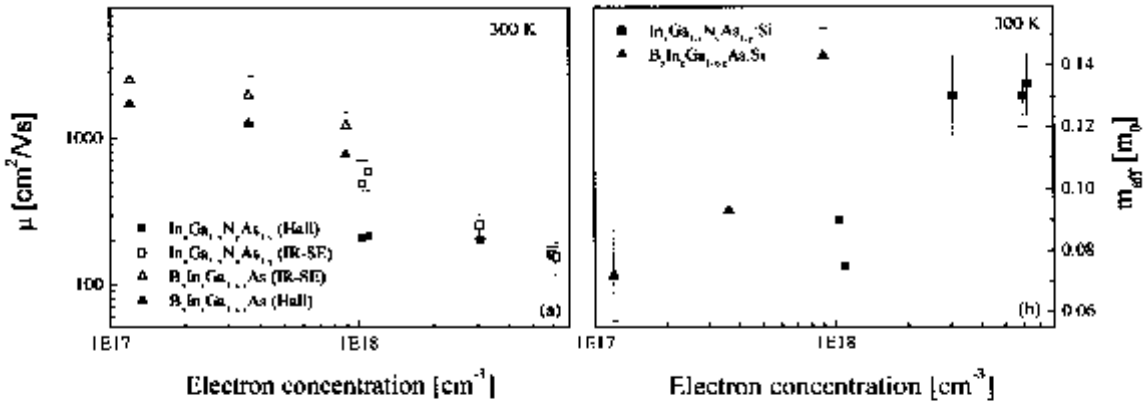

Fig. 3: (a): Mobilities of $In_xGa_{1-x}N_yAs_{1-y}$ (squares) and $B_xIn_zGa_{1-z}As$ (triangles) derived from Hall-measurements (solid symbols) and ellipsometry (open symbols). (b): Effective electron masses of $In_xGa_{1-x}N_yAs_{1-y}$ (squares) and $B_xIn_zGa_{1-z}As$ (triangles).

For the Si−doped layers, infrared spectroscopic ellipsometry was used to derive mobilities and effective masses using the Hall−concentrations as input parameter. Hall−mobilities and optically determined mobilities show in general the same trends (Fig. 3 (a)) and the effective masses increase for both materials with increasing carrier concentration (Fig. 3 (b)), which is an indicator of the nonparabolity of the conduction bands.

The room temperature PL−spectra of both materials are largely influenced by Si−doping as shown in Fig. 4. For $In_xGa_{1-x}N_yAs_{1-y}$ (a) and $B_xIn_zGa_{1-z}As$ (b), the maximum PL−intensities increase with increasing doping level up to ~ 10^{18} cm^{-3}. This effect is possibly caused by the interaction of the Si−dopants with other defects. For higher doping levels, the PL−intensities decrease in $In_xGa_{1-x}N_yAs_{1-y}$, which can be explained by defect creation due to

formation of Si−precipitates as observed in Si−GaAs [7].

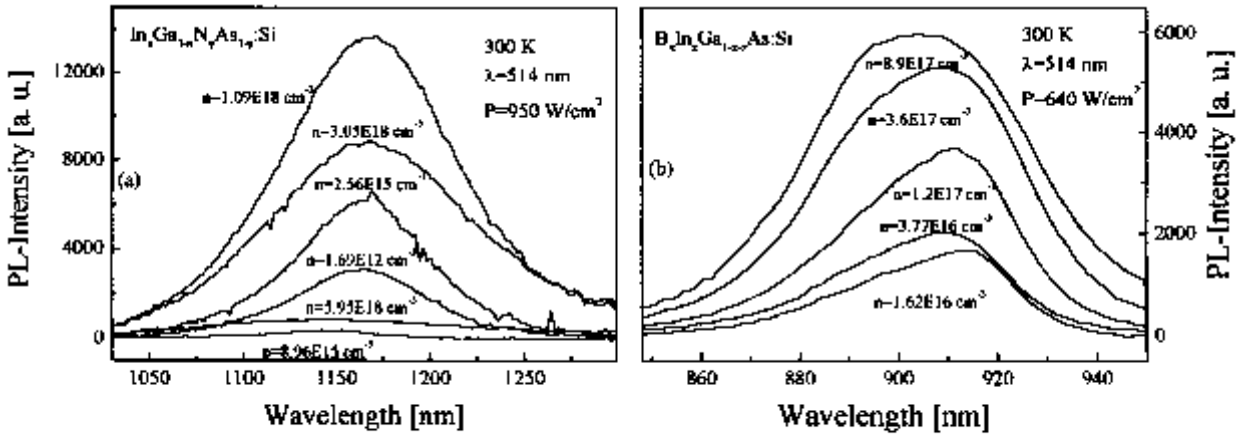

Fig. 4: Room temperature PL-spectra of $In_xGa_{1-x}N_yAs_{1-y}$ (a) and $B_xIn_zGa_{1-z}As$ (b).

Acknowledgement

This work was supported by BMBF under contract 03WKI07. We further acknowledge Mrs. U. Teschner and Dr. H. Herrenberger for considerable experimental support.

References

[1] M. Kondow *et al*., Jpn J. Appl. Phys. **35** (1996) 1273.

[2] K. Nakahara *et al*., IEEE Photonics Technol. Lett. **10** (1998) 487.

[3] D. J. Friedman et al., J. Cryst. Growth **195** (1998) 409.

[4] J. F. Geisz *et al*., Appl. Phys. Lett. **76** (2000) 1443.

[5] V. Gottschalch *et al*., J. Cryst. Growth **248** (2002) 468.

[6] K. Volz et al., J. Cryst. Growth **248** (2002) 451.

[7] X. Tang *et al*., J. Cryst. Growth **98** (1989) 827.